Cellular and Molecular Life Sciences (2024) 81:283
https://doi.org/10.1007/s00018-024-05315-y

ORIGINAL ARTICLE

Protein SUMOylation promotes cAMP-independent EPAC1 activation

Wenli Yang[1,2,3] · Fang C. Mei[1,2,3] · Wei Lin[1,2,3] · Mark A. White[4] · Li Li[3] · Yue Li[1,5] · Sheng Pan[1,3] · Xiaodong Cheng[1,2,3]

Received: 29 March 2024 / Revised: 20 May 2024 / Accepted: 12 June 2024

Abstract

Protein SUMOylation is a prevalent stress-response posttranslational modification crucial for maintaining cellular homeostasis. Herein, we report that protein SUMOylation modulates cellular signaling mediated by cAMP, an ancient and universal stress-response second messenger. We identify K561 as a primary SUMOylation site in exchange protein directly activated by cAMP (EPAC1) via site-specific mapping of SUMOylation using mass spectrometry. Sequence and site-directed mutagenesis analyses reveal that a functional SUMO-interacting motif in EPAC1 is required for the binding of SUMO-conjugating enzyme UBC9, formation of EPAC1 nuclear condensate, and EPAC1 cellular SUMOylation. Heat shock-induced SUMO modification of EPAC1 promotes Rap1/2 activation in a cAMP-independent manner. Structural modeling and molecular dynamics simulation studies demonstrate that SUMO substituent on K561 of EPAC1 promotes Rap1 interaction by increasing the buried surface area between the SUMOylated receptor and its effector. Our studies identify a functional SUMOylation site in EPAC1 and unveil a novel mechanism in which SUMOylation of EPAC1 leads to its autonomous activation. The findings of SUMOylation-mediated activation of EPAC1 not only provide new insights into our understanding of cellular regulation of EPAC1 but also will open up a new field of experimentation concerning the cross-talk between cAMP/EPAC1 signaling and protein SUMOylation, two major cellular stress response pathways, during cellular homeostasis.

Keywords SUMO · SUMO-interacting motif · Biomolecular condensate · Heat shock · Molecular dynamics

Introduction

Posttranslational modification with small ubiquitin-related modifier (SUMO) proteins is an essential and widespread regulatory mechanism for cellular homeostasis [1]. A significant portion of the human proteome has been identified to undergo SUMO modifications [2]. These SUMOylated proteins are involved in virtually all known cellular processes, including cell division, chromosome segregation, DNA replication/repair, gene transcription, nuclear transport, and signal transduction [1]. SUMOylation regulates these cellular processes by altering the target protein's activity, localization, stability, or interacting ability with binding partners [3]. SUMOylation has long been associated with stress responses, integrating a diverse array of cellular stress signals that trigger rapid changes in global protein SUMOylation [4–7]. Dysregulation of cellular SUMOylation has been implicated in the development of human diseases such as atherosclerosis, autoimmune diseases, cancer, diabetes, heart failure, and neurological disorders [8].

Wenli Yang and Fang C. Mei contributed equally.

✉ Xiaodong Cheng
xiaodong.cheng@uth.tmc.edu

1 Department of Integrative Biology and Pharmacology, The University of Texas Health Science Center, Houston, TX, USA

2 Texas Therapeutics Institute, The University of Texas Health Science Center, Houston, TX, USA

3 Brown Foundation Institute of Molecular Medicine, The University of Texas Health Science Center, Houston, TX, USA

4 Department of Biochemistry and Molecular Biology, Sealy Center for Structural Biology and Molecular Biophysics, The University of Texas Medical Branch at Galveston, Galveston, TX, USA

5 Present Address: Cell Therapy Manufacturing Center, 2130 W Holcombe Blvd, Houston, TX 77030, USA

Published online: 04 July 2024

In parallel, the cAMP second messenger is a primary stress-response signal that plays essential roles in diverse biological functions under physiological and pathophysiological conditions. In multi-cellular organisms, the effects of cAMP are mainly transduced by two ubiquitously-expressed intracellular cAMP receptor families, the cAMP-dependent protein kinase (PKA) and the exchange protein directly activated by cAMP (EPAC) [9, 10]. Between EPAC isoforms, EPAC1 and EPAC2, EPAC1 is ubiquitously expressed in all tissues, while EPAC2 has a limited tissue distribution, detected predominantly in the brain, pancreas, and adrenal gland [11, 12]. Despite acting on the same immediate down-stream effectors, the Ras superfamily small GTPases Rap1 and Rap2, cellular functions of EPAC1 and EPAC2 are frequently non-redundant due to their distinct tissue distribution and the ability to form discrete signalosomes at various cellular loci through interaction with specific cellular partners [13–16]. Although protein SUMOylation and EPAC signaling were discovered around the same time more than two decades ago, crosstalk between cAMP/EPAC signaling and protein SUMOylation, two central cellular stress-response mechanisms, has not been explored extensively. Our recent study demonstrated that cAMP acts through EPAC1 to promote cellular SUMOylation via regulating the formation of biomolecular condensates enriched with SUMO processing enzymes and substrates, connecting the two major stress-response pathways [17]. However, attempts to determine whether EPAC1 can undergo SUMO modification have not been successful. Consequently, the effects of EPAC1 SUMOylation remain unknown. In this study, we describe a novel finding that EPAC1 is a SUMO target protein and that SUMOylation of EPAC1 promotes its guanine exchange activity in a cAMP-independent manner.

Results

EPAC1 contains SUMO-consensus motifs (SCMs) and can be SUMOylated in cells

Many SUMO-modified proteins contain acceptor lysines within a ΨKX[D/E] SCM or an inverted ([E/D]XKΨ) SCM, where Ψ is a large hydrophobic amino acid, and X is any amino acid [18]. When the human EPAC1b sequence was analyzed using a SUMOylation prediction algorithm [19], several putative SCMs and a SUMO-interacting motif (SIM) [20, 21] were identified (Table S1). To test if EPAC1 is SUMOylated in cells, we subjected cells to heat shock treatment, known to induce robust cellular SUMOylation [6]. We subsequently probed the status of EPAC1, endogenously in Human Umbilical Vein Endothelial Cells (HUVECs) or ectopically expressed in HEK293 cells, which express a very low level of in-house EPAC1 [9], by immunoblotting using a monoclonal EPAC1 antibody, 5D3. Incubation of HUVECs or HEK293/EPAC1-Flag cells at 43 °C led to time-dependent accumulation of higher molecular weight EPAC1 immunoblotting signals above the ~ 100 kD EPAC1 native protein band (Fig. 1A, B). Similar results were obtained in HeLa cells transfected with an EPAC1-Flag/HA containing pOZ vector [22] (Supplementary Fig. 1A). Importantly, when cell lysates were treated with Sentrin-specific protease 1 (SENP1), a deSUMOylation protease, the higher molecular weight EPAC1 immunoblotting signals were markedly reduced (Fig. 1C, Supplementary Fig. 1B), suggesting that some of these higher molecular weight EPAC1 post-translational modification (PTM) signals are indeed originated from SUMOylated EPAC1.

Identification of an EPAC1 SUMOylation site by mass spectrometry (MS)

Encouraged by the finding of heat shock-induced, SENP1-sensitive EPAC1 PTMs, we mapped potential SUMOylation sites in EPAC1. Site-specific identification of SUMOylation by MS remains technically challenging owing to the dynamic nature of cellular SUMOylation [23] and the lack of naturally occurring tryptic sites near the C-terminal tail of SUMO proteins, unlike in the case of ubiquitin [2]. To overcome these challenges, we mutated the Q89 residue of SUMO3 to K so that tryptic digestion of conjugated SUMO3(Q89K) would leave a "signature peptide" containing a TGG adduct attached to the SUMOylated lysine on the substrate, allowing robust and unambiguous identification of the SUMOylation site using MS. We ectopically expressed the EPAC1-His_{10} and SUMO3(Q89K) in HEK293 cells simultaneously using a bicistronic lentivector and performed denaturing His-tag pull-down using lysate from cells treated with or without 30 min 43 °C heat shock (Fig. 2A). Immunoblotting analysis of the pull-down samples using an anti-SUMO2/3 antibody revealed that heat shock treatment led to a robust increase in SUMO2/3-containing high molecular weight bands (Fig. 2B). These results further support that EPAC1 can be SUMOylated, and heat shock promotes EPAC1 SUMOylation. MS analysis of the His-tag pull-down eluent of the heat shock sample led to the unambiguous identification of the K561 as a SUMOylation site in EPAC1 with a less than 1% false discovery rate (FDR) (Fig. 2C). The overall MS data quality was excellent with a sequence coverage for EPAC1 more than 90%. The MS spectra for peptides spanning the K561 were all high quality, both for modified and unmodified peptides. This allowed us to estimate the stoichiometry of K561 SUMOylation at ~ 9% based on the PSM (peptide-spectrum match) counts.

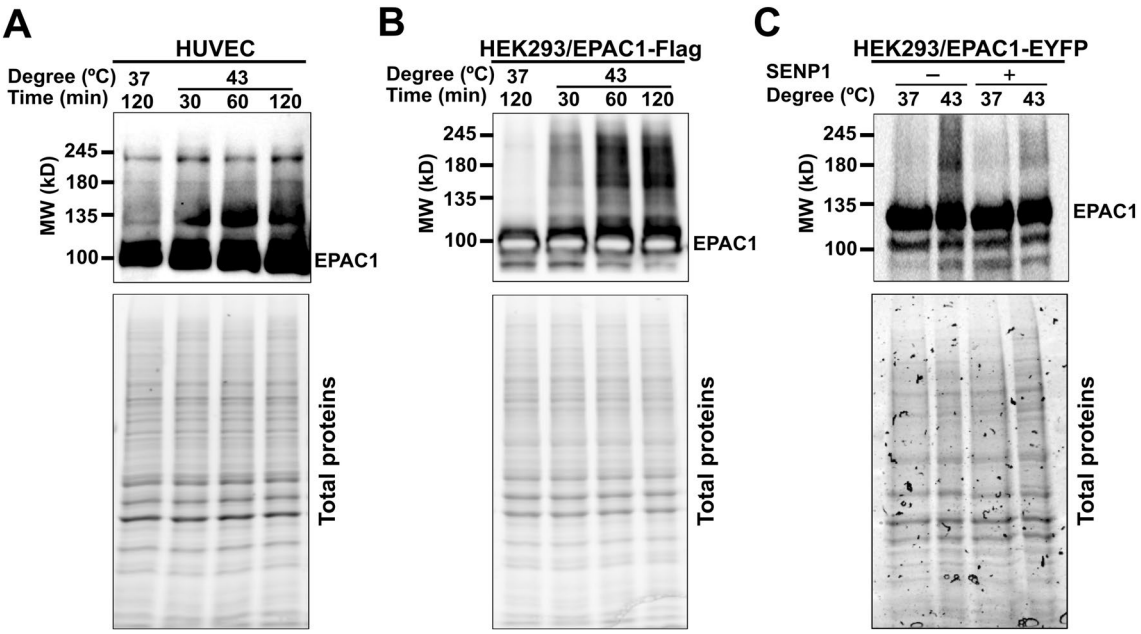

Fig. 1 Heat shock promotes EPAC1 post-translational modifications (PTM). Levels of cellular EPAC1 PTM probed by immunoblotting using anti-EPAC1 antibody in HUVEC (**A**) and HEK293/EPAC1-Flag **B** in response to heat shock as a function of time. **C** Levels of cellular EPAC1 PTM in HEK293/EPAC1-EYFP cells probed by immunoblotting using anti-EPAC1 antibody, with and without heat shock (30 min) and with or without SENP1 (220 nM) treatment at 37 °C for 20 min. Similar results were obtained from at least three independent experiments

An EPAC1 SUMO interacting motif (SIM) is required for EPAC1 SUMO modification

Many SUMOylation substrates also contain SIM interacting with free or conjugated SUMO [20, 21]. In certain SUMOylation targets, the SUMO-binding property of the SIM contributes to substrate recognition and is critical for SUMOylation [24, 25]. Since EPAC1 has a well-defined SIM, ^{320}VVLVL^{324}, we conjectured that the EPAC1 SIM might play a role in EPAC1 SUMOylation. To test this hypothesis, we replaced the EPAC1 SIM motif, VVLVL, with alanines to generate the EPAC1(SIM/5A) mutant. Anti-SUMO2/3 affinity purification followed by EPAC1 immunoblotting showed that mutation of the EPAC1 SIM led to the complete abolishment of high molecular SUMOylated EPAC1 bands seen in WT EPAC1-APEX2 fusion under both normal and heat shock conditions (Fig. 3A). These results suggest that EPAC1 SIM is essential for EPAC1 SUMOylation.

Our recent study shows that EPAC1 interacts with components of the cellular SUMOylation machinery, including the SUMO-conjugating enzyme UBC9 [17]. To explore the mechanism of the SIM-dependent EPAC1 SUMOylation, we expressed and purified GST-tagged wild-type EPAC1 and SIM mutant EPAC1(V321A/V323A) recombinant proteins and used these proteins as baits to perform affinity pull-down of recombinant UBC9 that was auto-SUMOylated using purified UBA2/AOS1 and SUMO1. As shown in Fig. 3B, full-length WT EPAC1 could interact with SUMOylated or free UBC9. On the other hand, EPAC1(V321A/V323A) SIM mutant lost the ability to bind UBC9, the only known SUMO-conjugating enzyme.

cAMP is not essential for EPAC1 SUMO modification.

To determine if cAMP binding is necessary for heat-shock-induced EPAC1 SUMOylation, we used a well-characterized EPAC1 mutant, EPAC1(R279E), with a single point mutation of a conserved and critical residue, Arg279, that is required for cAMP-binding [9]. We ectopically expressed WT EPAC1-APEX2 and EPAC1(R279E)-APEX2 in HEK293 cells and performed affinity pull-down using anti-SUMO2/3 antibody. Immunoblotting analysis of the pull-down samples using an anti-EPAC1 antibody showed that EPAC1(R279E) mutant retained the capability of being SUMOylated in response to heat shock as WT EPAC1 (Supplementary Fig. 2). These results suggest that heat shock-mediated EPAC1 SUMOylation does not require cAMP binding.

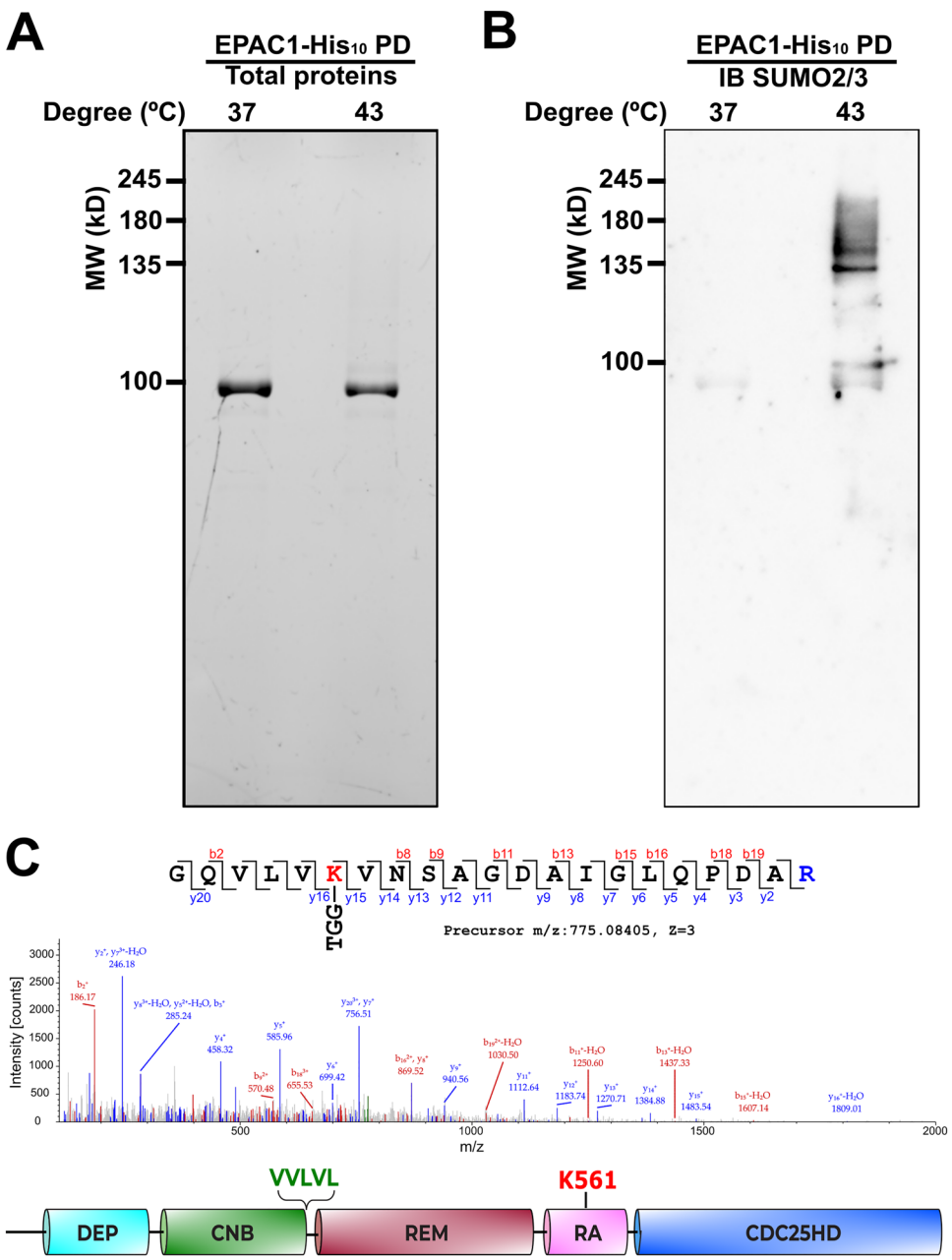

Fig. 2 EPAC1 is a SUMO target protein. Protein gel (**A**) and anti-SUMO2/3 immunoblotting (**B**) of nickel affinity pull-down of HEK293/pCDH-CMV-EPAC1-His_{10}-IRES-SUMO3(Q89K) lysates at 37 and 43 °C. **C** MS/MS spectrum and corresponding peptide sequence of EPAC1 SUMOylation site K561 (red). The domain structure of EPAC1 with a predicted SUMO-interacting motif is highlighted in green, and K561 is highlighted in red. *DEP* disheveled, *Egl-10* pleckstrin, *CNB* cyclic nucleotide binding, *REM* Ras exchange motif, *RA* Ras association, *CDC25HD* CDC25 homology domain

Biomolecular condensate, not RanBP2, is involved in heat shock-induced EPAC1 SUMOylation

EPAC1 interacts with RanBP2 [26, 27], a bona fide SUMO E3 ligase [28]. The close association between EPAC1 and RanBP2 raises the possibility that RanBP2 is involved in EPAC1 SUMOylation. However, when we performed the EPAC1 affinity pull-down experiment and probed the RanBP2, we found that heat shock led to a significant reduction of EPAC1 and RanBP2 interaction (Supplementary Fig. 3). This result suggests that RanBP2 is unlikely an E3 ligase that catalyzes the SUMOylation of EPAC1 in response to heat shock. On the other hand, we ectopically expressed EPAC1-EYFP and mRuby tagged ubiquitin-like modifier activating enzyme 2 (UBA2), the catalytic subunit of the SUMO E1 enzyme, in HEK293 cells and performed confocal imaging. At 37 °C, EPAC1-EYFP signals mainly were diffused. A few puncta were present in the cytosol but mostly absent in the nuclear compartment, while dispersed UBA2 speckles were observed in the nuclei. In response to heat shock stimulation, mRuby-UBA2 coalesced to form larger nuclear condensates. During this process, we also observed an increased formation of EPAC1-EYFP puncta, particularly in the nuclei that were superimposable with the mRuby-UBA2 in a time-dependent manner (Fig. 4A). Moreover, immunofluorescence staining of endogenous

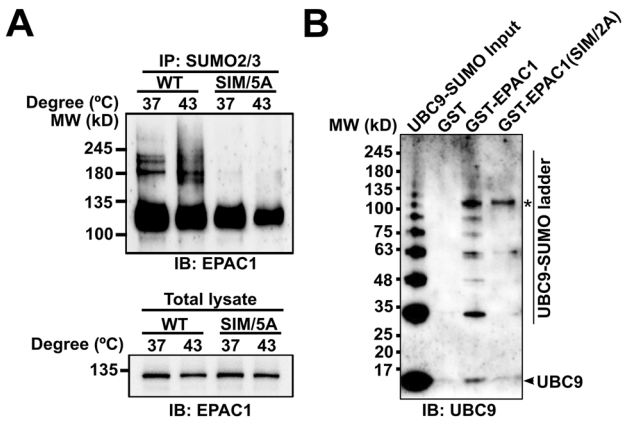

Fig. 3 SIM-dependent SUMOylation of EPAC1. **A** Anti-EPAC1 immunoblotting of SUMO2/3 affinity pull-down of HEK293/EPAC1-APEX2 and HEK293/EPAC1(SIM/5A)-APEX2 after incubation at 37 or 43 °C for 30 min. **B** Anti-UBC9 immunoblotting of GST, GST-EPAC1, and GST-EPAC1(V321A/V323A) pull-down of recombinant UBC9 protein auto-SUMOylated by SUMO1 in vitro. *indicates the GST-EPAC1 band

EPAC1and UBA2 in HUVEC revealed that heat shock stimulation (30 min) led to significant enhancement of EPAC1 and UBA2 nuclear signals and colocalization of EPAC1 and UBA2 nuclear puncta (Supplementary Fig. 4). These results, coupled with our previous findings that EPAC1 activation enhances cellular SUMOylation via promoting the formation of biomolecular condensates enriched with SUMOylation machinery [17], suggest that in addition to inducing SUMOylation promoting condensates, EPAC1 itself is a SUMO substrate during the process.

To further affirm the importance of nuclear condensate forming capability for heat-shock-induced EPAC1 SUMOylation, we tested the behavior of EPAC1(R279E)-EYFP and EPAC1(SIM/5A)-EYFP in response to heat shock. Our previous study shows that R279E mutation abolishes cAMP-induced EPAC1 nuclear condensates formation [17]. However, EPAC1(R279E)-EYFP, similar to WT EPAC1-EYFP, formed robust nuclear condensates that were superimposable with the mRuby-UBA2 condensates in response to heat shock (Fig. 4B). On the other hand, EPAC1(SIM/5A)-EYFP is mainly cytosolic. Mutation of the SIM abolished EPAC1's ability to form nuclear condensates in response to heat shock (Fig. 4C). The nuclear condensate formation capability of these mutants matched their SUMOylation status in response to heat shock, further supporting that nuclear condensates were involved in heat-shock-induced EPAC1 SUMOylation. Consistent with this notion, results based on cell fractionation analyses further revealed that heat shock-induced EPAC1 modification occurred mainly in the nuclear fraction (Supplementary Fig. 5). Furthermore, we tested the effect of K561R mutation on heat shock-induced EPAC1/UBA2 nuclear condensate formation. EPAC1(K561R) retains the ability to form nuclear condensates in response to heat shock as expected (Supplementary Fig. 6). These results suggest that EPAC1 SUMOylation at K561 is not required for heat shock-induced condensate formation.

EPAC1 contributes to heat-shock induced cellular SUMOylation

Our previous studies showed that EPAC1 activation by cAMP provokes cellular SUMOylation by promoting the formation of nuclear condensates enriched with EPAC1 and SUMO machinery. Our findings that heat shock, a known trigger of robust cellular SUMOylation [6], also led to the formation of EPAC1 and UBA2 containing condensates (Fig. 4) suggest that EPAC1 and heat shock mediated cellular SUMOylation share a similar mechanism, i.e., the formation of nuclear condensates enriched with SUMO machinery and that EPAC1 may play a role in heat-shock induced cellular SUMOylation. Indeed, heat shock-induced global SUMOylation was significantly reduced in HUVEC transfected with EPAC1-specific siRNAs compared to HUVEC cells treated with control siRNAs (Supplementary Fig. 7).

EPAC1 K561 SUMOylation is responsible for heat-shocked induced Rap GTPase activation

Protein SUMOylation is known to modulate the activity, stability, cellular localization, or interacting ability of the target protein [3]. To ascertain the functionality of EPAC1 K561 SUMOylation, we ask if K561 SUMOylation affects EPAC1's guanine nucleotide exchange activity. Since, under normal conditions, only a tiny fraction of EPAC1 is SUMOylated, we first tested if heat shock treatment, known to induce robust cellular SUMOylation, affected Rap1/2 activation. Figure 5A shows significant increases in heat shock-induced increases in both Rap1-GTP and Rap2-GTP levels as measured by a cellular Rap-GTP pull-down assay using a glutathione S-transferase fusion of the Rap1-binding domain of RalGDS that preferentially binds with GTP-bound Rap. To test if EPAC1 is responsible for the heat-shocked mediated Rap GTPase activation, we silenced EPAC1 expression via RNAi and compared heat shock-induced Rap activation in HUVECs cells treated with control or EPAC1-specific siRNAs. Knocking down EPAC1 blocked heat-shocked mediated Rap GTPase activation (Fig. 5B and C), suggesting that EPAC1 is a direct downstream effector of heat shock in terms of Rap activation.

To test if heat shock activates EPAC1 via increases in intracellular cAMP levels, we determined the intracellular cAMP concentration in HUVEC and HEK293 cells in

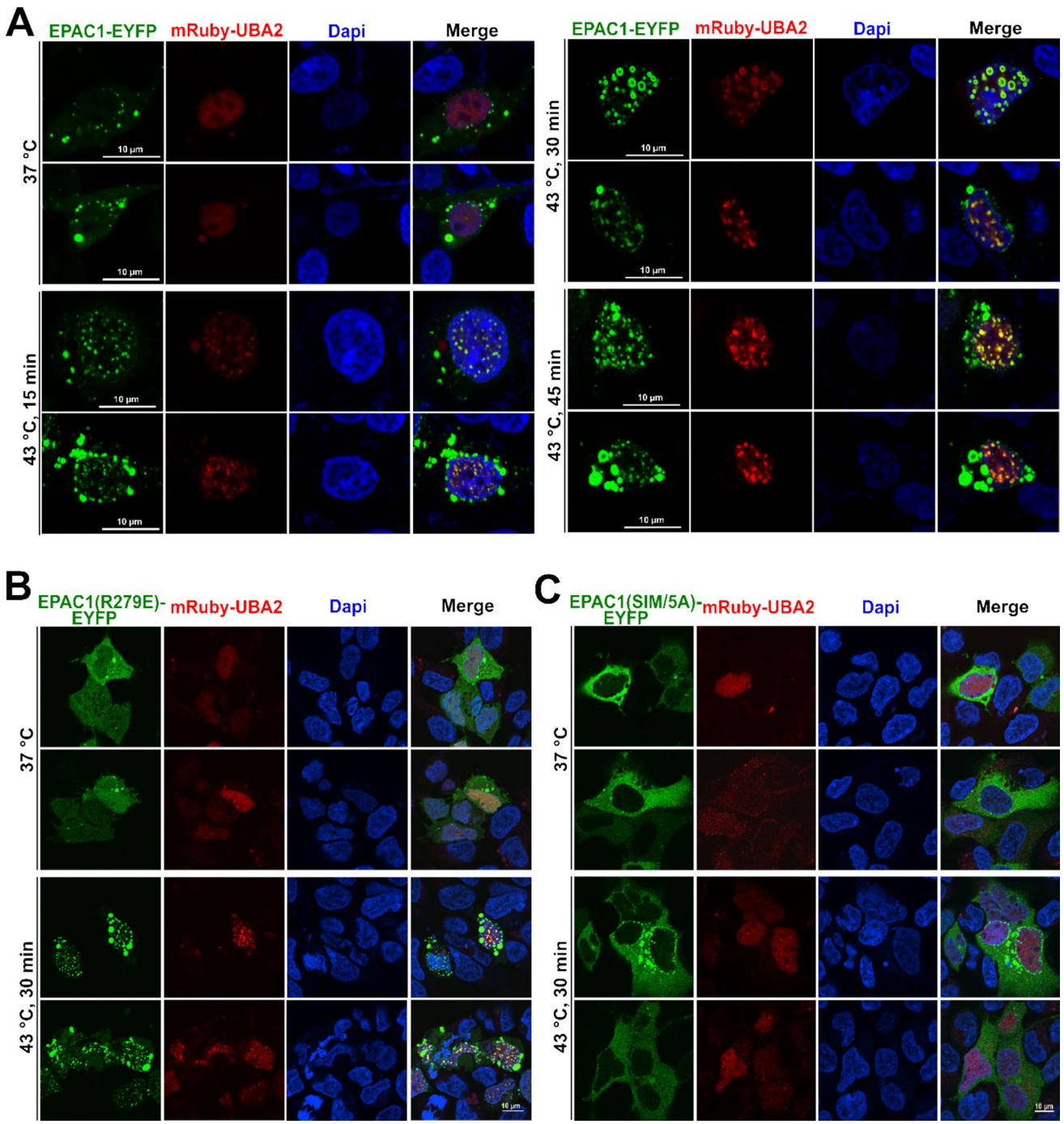

Fig. 4 Heat shock-induced formation of nuclear EPAC1-EYFP/mRuby-UBA2 condensates. **A** Confocal images of HEK293 cells ectopically expressing EPAC1-EYFP and mBuby-UBA2 in response to heat shock treatment as a function of time. Confocal images of HEK293 cells ectopically expressing EPAC1(R279E)-EYFP (**B**) or EPAC1(IM/5A)-EYFP (**C**) in response to heat shock treatment at 43 °C for 30 min. Bar = 10 μm

response to heat shock. Our data showed that heat shock did not significantly affect the intracellular cAMP levels in both cells (Supplementary Fig. 8). These findings led us to ask if EAPC1 K561 SUMOylation contributed to heat shock-induced Rap activation. When wild-type EPAC1-EYFP or an EPAC1(K561R)-YFP mutant was ectopically expressed in HEK293 cells, heat shock was able to promote Rap activation in HEK293/EPAC1-EYFP cells. However, this effect was abolished entirely in HEK293/EPAC1(K561R)-YFP cells (Fig. 6), suggesting that EPAC1 K561 SUMOylation

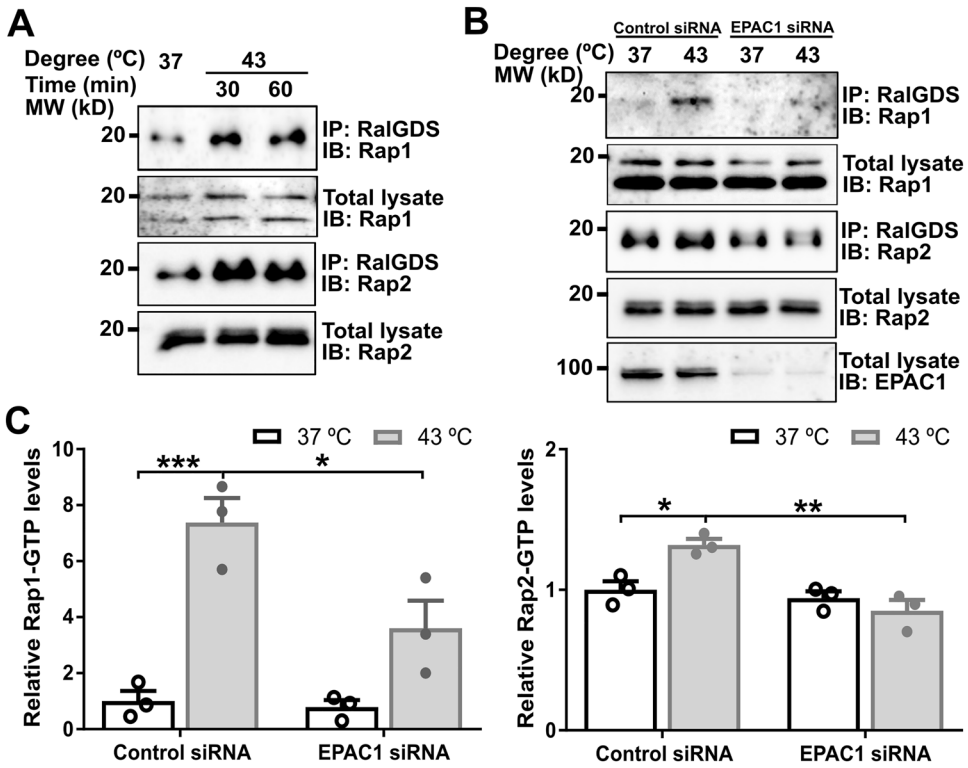

Fig. 5 EPAC1 is responsible for heat shock-induced activation of Rap small GTPases in HUVEC. **A** Heat shock promoted cellular activation of Rap1 and Rap2. **B** Silencing of EPAC1 abolished 30 min heat shock-induced Rap activation. **C** Quantification of cellular Rap1-GTP and Rap2-GTP levels in (**B**). Data are presented as Mean ± SEM (N = 3)

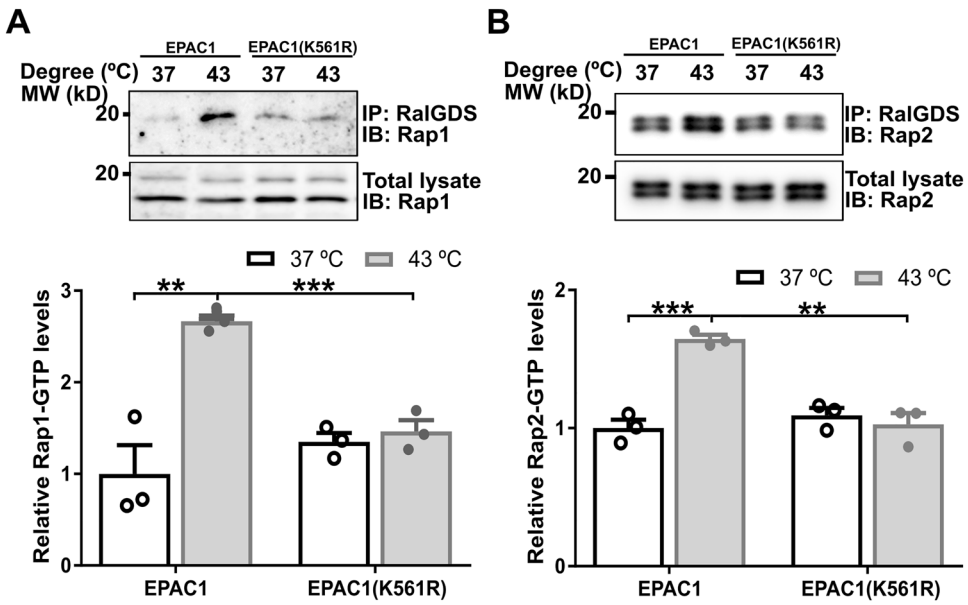

Fig. 6 K561 SUMOylation of EPAC1 is essential for heat shock-induced activation of Rap small GTPases. K561R mutation abolished heat shock-promoted cellular activation of Rap1 (**A**) and Rap2 (**B**). Data are presented as Mean ± SEM (N = 3)

is responsible for heat-shocked induced Rap GTPase activation.The finding that heat shock did not lead to changes in intracellular cAMP levels further supported the notion that cAMP was not required for heat shock-induced EPAC1 SUMOylation.

K561 SUMOylation of EPAC1 enhances Rap GTPase binding

To understand the structural basis of EPAC1(K561) SUMOylation mediated Rap GTPase activation, we performed structural modeling and molecular dynamics (MD) simulation analyses to generate K561 SUMOylated EPAC1 structures in apo

conformation (EPAC1(K561)-SUMO) or active conformation with the Rap1 effector bound (EPAC1(K561)-SUMO:cAMP:Rap1). Due to the presence of Rap1 in the active conformation, the possible position of the K561-SUMO moiety is restricted. In contrast, the initial position of the SUMO moiety is not restrained by its covalent bond to EPAC1 K561 in the apo conformation (Supplementary Fig. 9A). Despite this difference, the positions of the SUMO moiety of the two models remain similar after MD simulation with the SUMO orientation in EPAC1(K561)-SUMO shifted slightly in the absence of the Rap1 but remained in roughly the same position as in EPAC1(K561)-SUMO:cAMP:Rap1 (Supplementary Fig. 9B & C). The SUMO moiety seemed to position itself away from the N-terminal regulatory lobe (Supplementary Fig. 10A) and the Rap1 binding site in the CDC25HD domain, leaving it accessible for effector binding (Supplementary Fig. 9D). These results suggest that the SUMO moiety likely assumes a stable orientation before Rap1 binding. Analysis of the EPAC1(K561)-SUMO:cAMP:Rap1 revealed that the SUMO moiety moved slightly toward the bound Rap1 to make direct contact (Supplementary Fig. 9D). At the same time, the Rap1 rotated somewhat to accommodate the SUMO but remained securely bound to the EPAC1 CDC25HD domain (Supplementary Fig. 10B). In addition to the added interaction between SUMO and Rap1, the (K561)-SUMO substituent also increased the surface area between Rap1 and EPAC1 CDC25HD domain. As a consequence, the Rap1 footprint on the EPAC1(K561)-SUMO covered a significantly larger surface area of 2227 $Å^2$ (Fig. 7A and B) as compared to a buried surface area of 1486 $Å^2$ between Rap1 and EPAC1 alone (Fig. 7C and D).

Discussion

The universal second messenger, cAMP, is an ancient stress response signal conserved from bacterium to humans and is vital for optimal adaptation. Conversely, protein SUMOylation is a prevalent posttranslational modification essential for maintaining cellular homeostasis [29]. Recent studies demonstrate that cAMP, acting through EPAC1, can modulate cellular SUMOylation by promoting the formation of biomolecular condensate enriched with components of

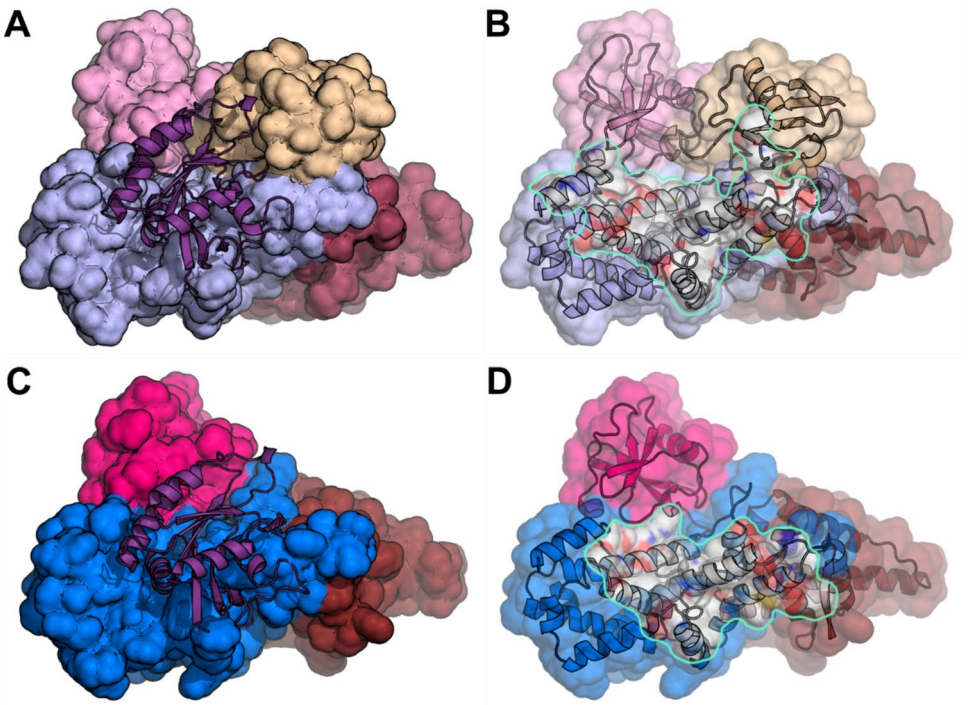

Fig. 7 K561 SUMOylation of EPAC1 promotes Rap1 interaction. **A** The MD $EPAC1^{CT}$-SUMO:Rap1 model after 30 ns of Molecular Dynamics showing the Rap1 (cartoon) bound to $EPAC1^{CT}$-SUMO. **B** The same view as in A with Rap1 removed and the Rap1 interface highlighted. The Rap1 total buried surface area is 2227 $Å^2$. **C** Corresponding view of the full-length EPAC1:cAMP:Rap1 model's catalytic domains after 30 ns of Molecular Dynamics showing the Rap1 (cartoon) bound to EPAC1 (For clarity, the regulatory domains are not shown). **D** The same view is seen in **C** with Rap1 removed and the Rap1 interface highlighted. The Rap1 total buried surface area is 1486 $Å^2$. The EPAC1 domains are colored as previously (REM: brown; RA: pink; CDC25HD: blue). The SUMO is beige, and the Rap1 is purple

SUMOylation machinery [17, 30]. These findings establish a crucial nexus linking two central cellular stress-response mechanisms. This study reveals that SUMOylation of EPAC1 on K561 of the Ras association (RA) domain enhances EPAC1 catalytic activity by providing an additional binding surface for its effector small GTPase Rap1/2. The unequivocal identification of a functional SUMOylation site in EPAC1 offers another mechanism connecting protein SUMOylation and cAMP signaling. It is worth noting that previous attempts to show SUMOylation of EPAC1 were not successful [27]. This is most likely because the level of cellular EPAC1 SUMOylation is very low and highly dynamic. To overcome this challenge, we ectopically expressd a mutant SUMO3(Q89K), coupled with heat shock to promote cellular SUMOylation. These modifications allow us to identify K561 as a primary SUMOylation site in EPAC1. It is important to note that while cAMP binding is not required for heat shock-induced EPAC1 K561 SUMOylation, the effect of cAMP binding on EPAC1 SUMOylation is unknown and remains to be determined.

Lysine 561 is located within the RA domain, which displays significant sequence diversity between the two EPAC isoforms [31]. RA domain folds into a ubiquitin alpha/beta roll superfold [32] and has been found in various proteins to function mainly as a protein interaction scaffold [33]. Previous studies have demonstrated that the RA domain contributes to isoform-specific functions of EPACs. RA domain in EPAC2 interacts with RAS and mediates EPAC2 translocation to the plasma membrane and activation [34–36]. A G706R rare coding mutation in the EPAC2 RA domain has been found in several autistic patients [37]. Functional analyses have revealed that G706R mutation impairs RAS interaction and selectively reduces basal dendrite complexity in cortical pyramidal neurons [38]. Conversely, the RA domain of EPAC1 is known to interact with β-arrestin2 and differentially regulates cardiac hypertrophic signaling mediated by β-adrenergic receptor subtypes [39]. In addition, EPAC1 RA has also been shown to mediate the interaction with Ran-GTP and RanBP2 proteins and to target EPAC1 to the nuclear membrane [26]. However, a subsequent study disputes the conclusions [27]. Our finding that SUMO modification of K561 in the EPAC1 RA domain enhances the interaction and activation of Rap GTPases further expands the role of RA domains in isoform-specific functions of EPACs. It will be interesting to test the effects of K561 SUMOylation on EPAC1's interaction with β-arrestin2 or RanBP2.

MD analyses of the EPAC1(K561)-SUMO revealed that the K561-SUMO moiety assumed a stable conformation without the effector, Rap1. In the presence of Rap1, the SUMO moiety moved slightly to make direct contact with the bound Rap1, which provided an extra binding interface to promote Rap1 binding to EPAC1(K561)-SUMO as compared to unmodified EPAC1. With SUMOylation, the measured Rap1 buried surface area increased from 1486 $Å^2$ to 2227 $Å^2$. Structural determination of SUMOylated proteins remains challenging due to lacking a general approach to produce recombinant proteins with site-specific SUMOylation. Our current study demonstrates that MD analysis is effective in interrogating EPAC1 SUMOylation to provide structural insights into SUMO modification.

In addition to being a SUMOylation substrate, EPAC1 also contains a well-defined SUMO-interacting motif. Interestingly, EPAC1 SIM, ^{320}VVLVL^{324}, overlaps with the "switchboard" (SB) sequence ^{321}VLVLE^{325} and is reported to be critical for maintaining the proper orientation between the regulatory and catalytic halves of EPAC1 [40]. Activation of EPAC1 by cAMP leads to a hinge motion that allows the translocation of the SB to become the "lid" of the cAMP binding pocket [41, 42]. Surprisingly, our study reveals that EPAC1 SIM is necessary for UBC9 interaction, the formation of heat-shock induced EPAC1 nuclear condensate, and EPAC1 SUMO modification, suggesting that it also acts as a switchboard for EPAC1 SUMOylation. The discovery that EPAC1 can be SUMOylated in cells and the identification of K561 as a primary EPAC1 SUMO modification site, coupled with the findings that EPAC1 contains a functional SIM, places EPAC1 among many known SUMO-interacting proteins that are themselves covalently SUMOylated [43]. The simultaneous presence of SUMO conjugation and SIM in single proteins can contribute to multivariant interactions essential for liquid–liquid phase separation (LLPS) and the formation of membraneless biomolecular condensates [29, 30, 44]. Considering the recent findings that EPAC1 contains intrinsically disordered domains and undergoes LLPS to form cellular condensates involved in the regulation of protein SUMOylation [17] and histone transcription [45], the ability of EPAC1 undergoing SUMO modification and interacting with SUMO-containing proteins provide additional mechanisms to regulate the assembly of large protein complexes/networks spatially and temporally via fine-tuning the phase separation of multivalent proteins.

Materials and methods

Reagents

Anti-EPAC1 antibody 5D3 (Cell Signaling Technology, #4155), anti-SUMO2/3 antibody (MBL Life Science, Catalog no. M114-3), anti-Ran BP2 antibody (Santa Cruz Biotechnology, Inc., Catalog no. sc-74518), Anti-Rap1 antibody (Santa Cruz Biotechnology, Inc., Catalog no. sc-65) and Anti-Rap2 antibody (BD Biosciences, Cat#

610215) were used in this study. Dulbecco's modified Eagle's medium (DMEM) high glucose (Catalog no. D5796), fetal bovine serum (FBS) (Catalog no. F2442), N-ethylmaleimide (NEM) (Catalog no. E3876), Ni Sepharose Fast Flow (Catalog no. GE17-5318), poly-l-lysine solution (0.01%, catalog no. P4707) and FluorSave Reagent (catalog no. 345789) were from MilliporeSigma. Antibiotic–antimycotic (100×) (Catalog no. 15240096), 4′,6-diamidino-2-phenylindole (DAPI) (Catalog no. 62248), and Lipofectamine 2000 (Catalog no. 11668-019) were from Thermo Fisher Scientific. cOmplete, Mini, EDTA-free Protease Inhibitor Cocktail Tablet was from Roche (catalog no. 11836170001). Protein A/G PLUS-Agarose (Catalog no. sc-2003) was from Santa Cruz Biotechnology Inc. Tris(2-carboxyethyl)phosphine hydrochloride (TCEP) (Catalog no. HR2-651) was from Hampton Research. Recombinant Human His6-SENP1 Catalytic Domain (SENP1, Catalog no. E-700) was from R&D Systems.

Constructs

Human EPAC1b protein C-terminally tagged with a Flag or EYFP was described previously [46]. pOZ-FH-C-EPAC1 construct encoding a C-terminal HA/Flag double epitope-tagged EPAC protein was previously described [22]. EPAC1-V5-APEX2 construct was generated by inserting the EPAC1 gene into the pCDNA3-V5-APEX2 vector [47] using NotI and NheI restriction enzyme sites. The EPAC1-V5-APEX2 fragment was linearized with EcoRI and NotI and cloned into the pCDH-CMV-MCS-EF1α-Puro (System Biosciences, Catalog no. CD510B-1) lentiviral vector. A bicistronic construct expressing human EPAC1b with a C-terminal His_{10} tag and SUMO3(Q89K) was constructed using the pIRES2-EGFP vector (Clontech Catalog no. 632435). The EPAC1-His_{10}-IRES-SUMO3(Q89K) fragment was linearized with EcoRI and NotI and cloned into the pCDH-CMV-MCS-EF1α-Puro lentiviral vector to generate the pCDH-CMV-EPAC1-His_{10}-IRES-SUMO3(Q89K) plasmid.

Recombinant protein expression and purification

Recombinant full-length human EPAC1b proteins were constructed as a Glutathione S-transferase (GST)-fusion, expressed in *Escherichia coli* CK600K cells and purified as described previously [48, 49]. Recombinant His_6-AOS1/UBA2, UBC9, SUMO1, and SUMO2/3 proteins were expressed and purified as described previously [50].

UBC9 in vitro SUMOylation and EPAC1-GST pulldown

SUMOyation of UBC9 was carried out by incubating 100 µg purified recombinant UBC9 with 6.7 µg AOS1-UBA2, 73 µg SUMO1, and 5 µM ATP in a reaction mixture containing 20 mM Tris, pH 8.0, 100 mM NaCl, 0.1 mM DTT, and 5 mM $MgCl_2$ at 37 °C. After 4 h of incubation, 50 µl of glutathione-agarose beads (50% slurry) with 38 µg purified GST-EPAC1 or GST-EPAC1(V321A/V323A) protein immobilized and equilibrated in buffer A (50 mM Tris, pH 7.1, 150 mM NaCl, 1 mM $MgCl_2$, 1 mM EDTA, 0.5% C12E9, 1 mM TCEP, 1× protease inhibitor) was added to 20 µl of UBC9 SUMOylation reaction mixture and incubated at 37 °C with gentle mixing for 45 min. The beads were washed twice with buffer A and three times with buffer B (same as buffer A except for 0.05% C12E9) and eluted with 20 mM reduced glutathione (GSH) in 45 µl buffer B.

SUMOylation site and SUMO-interacting motif prediction

Putative SUMOylation sites and SUMO-interacting motifs of human EPAC1b were analyzed using a web-based Joined Advanced SUMOylation Site and SIM Analyser (http://www.jassa.fr/) [19]. Candidates with "High cut-off" predictive scores or "DB hit" that matches a previously validated SUMOylation site, or SIM were selected as putative hits.

Cell culture, transfection, and HEK293/EPAC1-V5-APEX2 stable cell lines establishment

HEK-293 (ATCC, Catalog no. CRL-1573) and HeLa (ATCC, Catalog no. CCL-2) cells were grown in DMEM supplemented with 10% heat-inactivated FBS (Invitrogen) at 37 °C, 5% CO_2. HUVECs (Lonza, catalog no. C2519A) were maintained and subcultured in EGM-2 Endothelial Cell Growth Medium (Lanzo, catalog no. CC-3162) at 37 °C in a 5% CO_2 humidified incubator. Cell passages between 2 and 8 were used for experiments described in this study. For experiments involving RNA interference (RNAi), HUVECs at 70% confluence were transfected with EPAC1-specific (Thermo Fisher Scientific, Catalog no. 1299001) or non-targeting control Stealth RNAi siRNA oligonucleotides (Thermo Fisher Scientific, Catalog no. 12935300) at a final concentration of 50 nM. Cell transfection was performed using Lipofectamine 2000 according to the manufacturer's instructions. HEK-293 cells stably expressing EPAC1-V5-APEX2 were established using the MISSION Lentiviral Packaging Mix Production system (Sigma-Aldrich, catalog no SHP001 and SHP002). HEK293T cells at 70% confluence were transfected with pCDH-EPAC1–V5-APEX2,

pCDH-EPAC1(SIM/5A)–V5-APEX2 or pCDH-EPAC1(R279E)–V5-APEX2 lentiviral vectors and Lentiviral Packaging Mix for 48 h. Viral particles were harvested and used to infect HEK-293 cells for 48 h followed by selection using puromycin (2 µg/ml).

Heat shock-induced EPAC1 posttranslational modification (PTM)

Near-confluent HUVEC, HeLa/pOZ-FH-C-EPAC1 [22], and HEK293 cells ectopically expressing EPAC1-Flag or EPAC1-EYFP grown in 12-well plates were subjected to heat shock treatment at 43 °C for various periods. After treatment, cells were washed twice with warm Dulbecco's phosphate-buffered saline (DPBS) and lysed with 100 µl of 1 × SDS sample buffer [50 mM Tris (pH 6.8), 2% SDS, 0.1% bromophenol blue, 3% 2-ME, and 10% glycerol] with protease inhibitors and 20 mM NEM. Total cell lysates were collected and sonicated on ice using 15-W power output for three to four cycles of 5 s, with 5 s rests in between until entirely soluble. After heat denaturation at 95 °C for 5 min, the samples were subjected to immunoblotting analysis using an anti-EPAC1 antibody. To test if EPAC1 PTM was sensitive to SUMO-specific deconjugating enzyme, heat shock treated cells were lysed with 1 × cell lysis buffer without 20 mM NEM and then incubated with 220 nM recombinant Human Sentrin-specific protease 1 (SENP1) catalytic domain (R&D Systems, Catalog no. E-700) at 37 °C for 20 min before immunoblotting analysis.

Nickel affinity pull-down of HEK293/pCDH-CMV-EPAC1-His_{10}-IRES-SUMO3(Q89K) treated by HS

HEK-293 cells stably expressing EPAC1-His_{10} and SUMO3(Q89K) were generated using pCDH-CMV-EPAC1-His_{10}-IRES-SUMO3(Q89K) lentiviral vector and used for the in vivo identification of the EPAC1 SUMOylation site via nickel affinity purification under denaturing conditions using a well-established procedure as described previously [51]. Briefly, when eight 10 cm plates of HEK-293 cells stably expressing EPAC1-His_{10} and SUMO3(Q89K) reached 70%-80% confluence, four plates were subject to heat shock treatment at 43 °C for 30 min while the remaining four were kept at 37 °C. The cells were rinsed in PBS three times and lysed with 1 ml freshly prepared lysis buffer [10 mM Tris, 100 mM Sodium phosphate, pH 7.8, 400 mM NaCl, 6 M guanidine chloride, 20 mM imidazole, 0.5 mM EDTA, 0.5 mM PMSF, 10 mM NEM] directly on the plate. After gently rocking for 10 min, cell lysate was scrapped off, pooled, sonicated for 5 s, three times, on low power, and centrifuged at 16,000 g for 15 min to remove cell debris. The resultant supernatant was mixed with 45 µl of Sephorase 6 fast-flow nickel beads (GE 17-5318-02) equilibrated in the lysis buffer and incubated at room temperature with gentle mixing for three hours. The supernatant was carefully removed after centrifugation at 1000 g for 3 min. The remaining beads were washed twice with lysis buffer containing 0.1% TritonX-100, twice with freshly prepared pH 8.0 wash buffer [10 mM Tris, 100 mM sodium phosphate, pH 8.0, 8 M Urea, 0.1% (vol/vol) Triton X-100, 5 mM β-mercaptoethanol], and three times with freshly prepared pH 6.3 wash buffer [10 mM Tris, 100 mM sodium phosphate, pH 6.3, 8 M Urea, 0.1% (vol/vol) Triton X-100, 5 mM β-mercaptoethanol]. EPAC1-His_{10} was eluted from the beads with elution buffer [150 mM Tris–HCl pH 6.7, 300 mM Imidazole, 5% (wt/vol) SDS, 30% (vol/vol) glycerol, 5 mM β-mercaptoethanol]. The eluents were loaded onto 10% SDS-polyacrylamide gel electrophoresis (SDS-PAGE) gel. Shortly after all the eluents were migrated into the gels, gel bands (1 to 2 cm) containing the total protein loading were excised after staining with Coomassie Blue. The gel bands were subjected to in-gel tryptic digestion as previously described [52].

LC/MS/MS analysis

An aliquot of the tryptic digest (in 2% acetonitrile/0.1% formic acid in water) was analyzed by LC/MS/MS using an Orbitrap Fusion™ Tribrid™ mass spectrometer (Thermo Scientific™) interfaced with a Dionex UltiMate 3000 Binary RSLCnano System. Peptides were separated with a C18 reversed-phase column (100 µm ID × 25 cm, 5 µm/18 Å Reprosil-Pur C18-AQ beads from Dr Maisch, Ammerbuch-Entringen, Germany) at a flow rate of 350 nl/min. Gradient conditions were: 3%–22% B for 40 min, 22%–35% B for 10 min, 35%–90% B for 10 min, followed by 90% B for 10 min (solvent A, 0.1% formic acid in water; solvent B, 0.1% formic acid in acetonitrile). The peptides were analyzed using a data-dependent acquisition mode. The survey scan was performed with 120 K resolution from 350 to 1500 m/z with an AGC target of 2e5 and a max injection time of 50 ms. The DDA cycle was limited to 3 s. Monoisotopic masses were then selected for further fragmentation for ions with 2 to 5 plus charge within a dynamic exclusion range of 20 s. Fragmentation priority was given to the most intense ions. Precursor ions were isolated using the quadrupole with an isolation window of 1.6 m/z. HCD was applied with a normalized collision energy of 34%, and resulting fragments were detected using the rapid scan rate in the ion trap. The AGC target for MS/MS was set to 1e4, and the maximum injection time was limited to 35 ms.

The raw data files were processed using Thermo Scientific™ Proteome Discoverer™ software. The spectra were searched against the Uniprot-Homo sapiens database

using Sequest. The database search was restricted to the following parameters. Trypsin was set as the enzyme with maximum missed cleavages set to 2. The precursor ion tolerance was set to 10 ppm, and the fragment ion tolerance was set to 0.8 Da. Carbamidomethylation on cysteine was selected as a static modification. Variable modifications were set to oxidation of methionine, acetylation of N-terminus, ubiquitination of Lysine (Gly-Gly), and SUMOylation of Lysine (T-Gly-Gly). The search results were validated and trimmed to a 1% FDR for strict conditions and 5% FDR for relaxed conditions using Percolator.

Monitoring cellular SUMOylation of EPAC1 by SUMO2/3 affinity pull-down

HEK293/EPAC1-APEX2, HEK293/EPAC1(SIM/5A)-APEX2 or HEK293/EPAC1(R279E)-APEX2 cells with 80–90% confluence were subject to heat shock treatment at 43 °C for 30 min, while control cells were kept at 37 °C. For each condition, two 10 cm plates were used. The cells were rinsed with cold PBS and lysed in lysis buffer containing 50 mM Tris (pH 7.5), 150 mM NaCl, 1.5 mM $MgCl_2$, 0.5 mM EDTA, 20 mM NEM, 1 mM phenylmethylsulfonyl fluoride (PMSF), 1% NP-40, and 1 × cOmplete Protease Inhibitor Cocktail on ice for 5 to 10 min. Cell lysates were harvested by centrifugation at 16,000 g for 15 min to remove cell debris. Cell lysates with an equal amount of total cellular proteins (1.6 mg) were incubated with 3 µg of anti-SUMO2/3 antibody (Catalog no. M114-3, MBL Life Science) or mouse immunoglobulin G (IgG) (Catalog no. sc-2025, Santa Cruz Biotechnology) with gentle mixing at 4 °C for 2 h. Protein A/G PLUS-Agarose beads (20 µl), equilibrated in lysis buffer, were added to the sample mixtures and incubated at 4 °C with gentle mixing for 1 h. The agarose beads were collected by centrifugation at 1000 g for 3 min and washed five times with buffer containing 50 mM Tris (pH 7.5), 150 mM NaCl, 1.5 mM $MgCl_2$, 0.5 mM EDTA, 20 mM NEM, 1 mM PMSF, 0.75% NP-40, and 5% glycerol. After the final wash, the beads were resuspended in 40 µl of 2 × SDS sample buffer. The SUMO2/3 immunoprecipitation samples were analyzed by SDS-PAGE and immunoblotting using anti-EPAC1 antibody 5D3 (Catalog no. 4155, Cell Signaling Technology).

Cell fractionation of heat shock-induced EPAC1 posttranslational modification (PTM)

Near-confluent HEK293 cells ectopically expressing EPAC1-Flag grown in 6 cm culture dish were subjected to heat shock treatment at 43 °C for 30 min. After treatment, cells were washed with ice-cold Dulbecco's phosphate-buffered saline (DPBS), scraped from culture dishes on ice using a plastic cell scraper and collected in 1.5 ml tubes in 1 ml ice-cold PBS buffer. After centrifugation at 500 g for 5 min, supernatants were removed, and cell pellets were resuspended in 400 µl of cytoplasmic lysis buffer (0.15% NP-40, 150 mM NaCl, 1 × cOmplete protease inhibitor, 0.5 mM EDTA, 20 mM NEM, 1 mM PMSF), incubated on ice for 5 min. 60 µl of the lysate was removed as whole cell lysate and mixed with 20 µl of 4 × SDS sample buffer, then kept on ice until the sonication step. The remaining lysate was centrifuged at 1000 g for 5 min, and 120 µl of the supernatant was removed as the cytosolic fraction, mixed with 40 µl of 4 × SDS sample buffer, and boiled for 1 min. After the remaining supernatant was removed, the pellet was resuspended in 500 µl of nuclei wash buffer (phosphate-buffered saline containing 0.1% Triton X-100, 1 mM EDTA, 1 × complete protease inhibitor, 20 mM NEM, 1 mM PMSF) and centrifuged at 1000 g for 2 min and the supernatant was discarded. The wash step was repeated one time. The pellet was resuspended with 80 µl of 1 × SDS sample buffer and designated as nuclear fraction. The whole cell lysate and nuclear fraction were sonicated twice for 5 s each and then boiled for 1 min. 10 µL, 10 µL, and 5 µL of whole cell lysate, cytoplasmic, and nuclear fractions, respectively, were loaded and separated using SDS-PAGE. The signals of EPAC1 PTM, α-Tubulin, and Lamin B were detected by Western Blot using anti-EPAC1 (Cell Signaling Technology), anti-α-Tubulin (Cell Signaling Technology), and anti-Lamin B (Santa Cruz Biotechnology Inc.) antibodies.

Immunofluorescence staining and confocal imaging analysis

HEK293 cells were plated on glass coverslips coated with 2% gelatin or poly-l-lysine (10 µg/ml) and transfected with EPAC1-EYFP, EPAC1(R279E)-EYFP, EPAC1(SIM/5A)-EYFP or EPAC1(K561R)-EYFP and pcDNA-mRuby-UBA2. Twenty-four hours post-transfection, the cells were subjected to heat shock treatment at 43 °C for various time points, fixed with 4% PFA for 20 min at 37 °C, rinsed three times with PBS for 5 min each, and stained with DAPI solution. Coverslips were mounted with FluorSave reagent for fluorescence microscopic imaging with a Nikon AXR or A1R laser confocal microscope system using the same parameter settings, including the laser power and exposure time. Images for more than eight randomly selected fields from at least three independent coverslips per treatment condition were collected. Immunofluorescence staining of endogenous EPAC1 and UBA2 in HUVEC cells was performed using anti-EPAC1 (1:200; Santa Cruz Biotechnology Inc., catalog no. SC-25632), anti-UBA2 (1:250; Santa Cruz Biotechnology Inc., catalog no.

SC-376305) antibodies and as previously described [17]. Fluorescence microscopic images were captured using a Nikon AXR confocal microscope system.

Intracellular cAMP determination

The intracellular cAMP levels of HUVEC or HEK-293 cells with or without heat shock treatment were measured using a Direct cAMP ELISA kit from Enzo Biochem (Catalog no. AD1-900-066A) following the manufacturer's instructions and normalized using total using cellular protein concentration.

Cellular Rap-GTP pull-down assay

The cellular activities of Rap1 and Rap2 in HUVEC or HEK293 cells ectopically expressing EPAC1-EYFP or EPAC1(K561R)-YFP were assessed using a glutathione S-transferase fusion of the Rap1-binding domain of RalGDS as described earlier [9]. Briefly, cells were grown to 75% confluence in a 10-cm Corning culture dish and subjected to heat shock treatment at 43 °C for 30 min while control cells were kept at 37 °C. Following three washes in PBS, the cells were lysed in a buffer containing 50 mM Tris (pH 7.5), 150 mM NaCl, 2.5 mM $MgCl_2$, 0.5% Na-deoxycholate, 0.1% SDS, 20 mM NEM, 1 mM PMSF, 1% NP-40, and 1 × Roche EDTA-free protease inhibitors. The cell lysate was mixed with 30 µl of glutathione-Sepharose beads with 30 µg of glutathione S-transferase-RalGDS-Rap1-binding domain bound and incubated at 4 °C for 2 h with gentle agitation. Following five washes in lysis buffer, the beads were suspended in 40 µl of SDS sample buffer. 10–15 µl of protein samples were loaded onto a 15% SDS-polyacrylamide gel and further analyzed with Western blot using Rap1 and Rap2 specific antibodies.

Molecular modeling and dynamics simulation analyses of K561-SUMOylated EPAC1

The Rap1 bound EPAC1 structure was based on a published EPAC1 model based on homology modeling and rigid-body and ensemble analyses of Small-Angle X-ray Scattering (SAXS) data [53]. In brief, the EPAC2:cAMP:Rap1 3CF6 PDB structure was used as the template for generating an EPAC1:cAMP:Rap1 model using Modeller [54]. The SUMO molecule from the 3UIP structure was extracted and positioned near K561 of EPAC1 using Pymol. The linkage between the SUMO di-glycine terminus and EPAC1 K561 was made in COOT. The SUMO:EPAC1 interface residues were energy minimized with stereochemical restraints in COOT [55]. This starting model was prepared for NAMD [56] using the VMD solvation and autoionization modules [57] using a 30 Å padded box with a 150 mM NaCl concentration. The solvated model was then minimized and annealed in NAMD before performing a Molecular Dynamics Simulation run of 30 ns. These were performed using an NPT ensemble and PME electrostatics with a 12 Å cutoff and 10 Å switching distance. We performed three MD Simulations to probe the SUMOylated EPAC1 Rap1 effector binding system. For the EPAC1-SUMO:Rap1 model. The choice of an initial position of the SUMO in the EPAC1:cAMP:Rap1 receptor-bound complex is highly restricted due to steric hindrance. The SUMO was manually positioned in a cleft between the Rap1 and the RA domain of EPAC1 in the only possible orientation, one in which the EPAC1 N-terminal regulatory domains were distal to the SUMO and could not interact. Therefore, the MD Simulations were performed with the EPAC1 C-terminal domains ($EPAC1^{CT}$) that span K561 by truncating the N-terminal regulatory domains. For the $EPAC1^{CT}$-SUMO model, the initial position of the SUMO relative to the $EPAC1^{CT}$ domains is not restrained by its covalent bond to K561 of EPAC1. The $EPAC1^{CT}$-SUMO model was derived from a minimized and annealed $EPAC1^{CT}$-SUMO:Rap1 model with the Rap1 effector removed. This gave the SUMO an initial orientation to the $EPAC1^{CT}$ domains, which was physically reasonable. The MD Simulation run of this $EPAC1^{CT}$-SUMO model probes whether this was a stable orientation that may be adopted before receptor binding or if the SUMO would move from this position. The third simulation was performed on the full-length ternary EPAC1:cAMP:Rap1 homology model reported previously [53]. The resulting ternary model was used for comparative analysis with the SUMOylated model. This full-length ternary model after MD improved fitting to the experimental SAXS data, validating the effectiveness of the MD analyses.

Statistical analyses

Results are presented as mean ± standard error of the mean (SEM). Data was analyzed for normality and equal variance using the Shapiro–Wilk normality test and an F-test, respectively. For data exhibiting normal distribution, a Student t-test was implemented to compare two groups of equal variances, whereas a Welch t-test was used in cases with unequal variance. For non-normal distributions, a Mann–Whitney test was conducted to compare groups. Additionally, one-way ANOVA with a Bonferroni post hoc test was used to compare groups of three or more with normal distributions. A p-value less than 0.05 was considered statistically significant.

Supplementary Information The online version contains supplementary material available at https://doi.org/10.1007/s00018-024-05315-y.

Author Contributions Wenli Yang: Methodology; Investigation; Validation; Formal analysis; Data Curation; Writing-Method, Review & Editing; Visualization. Fang Mei: Methodology; Investigation; Validation; Formal analysis; Data Curation; Writing-Review & Editing; Visualization. Wei Lin: Methodology; Investigation; Validation; Data Curation; Writing-Method. Mark White: Methodology; Investigation; Validation; Formal analysis; Data Curation; Writing-Method, Review & Editing; Visualization. Li Li: Methodology; Investigation; Validation; Formal analysis; Data Curation; Writing-Method, Review & Editing. Yue Li: Methodology; Resources. Sheng Pan: Data Curation; Writing-Method, Review & Editing. Xiaodong Cheng: Conceptualization; Methodology; Investigation; Validation; Formal analysis; Resources; Data Curation; Writing-Original draft preparation, Review & Editing; Visualization; Supervision; Project administration; Funding acquisition.

Funding Grants from the National Institutes of Health R35GM122536 and the American Heart Association 20TPA35410051 supported this work. The authors thank the Clinical and Translational Proteomics Service Center at the University of Texas Health Science Center at Houston for the proteomic analysis and Dr. Olga Chumakova and Ms. Zhengmei Mao from UTHealth Center for Advanced Microscopy for technical assistance. The authors acknowledge the Sealy Center for Structural Biology and Molecular Biophysics at the University of Texas Medical Branch at Galveston for providing research resources. The funders had no role in the study design, data collection and analysis, publication decision, or manuscript preparation.

Availability of data and material Data and material will be available upon request.

Declarations

Conflict of interest The authors declare no competing financial interests.

Ethical approval and consent to participate Not applicable. This study does not involve human subjects or animals.

Consent for publication Not applicable. This study does not involve human subjects and personal data.

References

1. Flotho A, Melchior F (2013) Sumoylation: a regulatory protein modification in health and disease. Annu Rev Biochem 82:357–385. https://doi.org/10.1146/annurev-biochem-061909-093311
2. Hendriks IA, Vertegaal AC (2016) A comprehensive compilation of SUMO proteomics. Nat Rev Mol Cell Biol 17:581–595. https://doi.org/10.1038/nrm.2016.81
3. Geiss-Friedlander R, Melchior F (2007) Concepts in sumoylation: a decade on. Nat Rev Mol Cell Biol 8:947–956. https://doi.org/10.1038/nrm2293
4. Saitoh H, Hinchey J (2000) Functional heterogeneity of small ubiquitin-related protein modifiers SUMO-1 versus SUMO-2/3. J Biol Chem 275:6252–6258. https://doi.org/10.1074/jbc.275.9.6252
5. Zhou W, Ryan JJ, Zhou H (2004) Global analyses of sumoylated proteins in *Saccharomyces cerevisiae*. Induction of protein sumoylation by cellular stresses. J Biol Chem 279:32262–32268. https://doi.org/10.1074/jbc.M404173200
6. Golebiowski F, Matic I, Tatham MH, Cole C, Yin Y, Nakamura A, Cox J, Barton GJ, Mann M, Hay RT (2009) System-wide changes to SUMO modifications in response to heat shock. Sci Signal 2:24. https://doi.org/10.1126/scisignal.2000282
7. Yang W, Thompson JW, Wang Z, Wang L, Sheng H, Foster MW, Moseley MA, Paschen W (2012) Analysis of oxygen/glucose-deprivation-induced changes in SUMO3 conjugation using SILAC-based quantitative proteomics. J Proteome Res 11:1108–1117. https://doi.org/10.1021/pr200834f
8. Chang HM, Yeh ETH (2020) SUMO: From Bench to Bedside. Physiol Rev 100:1599–1619. https://doi.org/10.1152/physrev.00025.2019
9. Mei F, Qiao J, Tsygankova O, Meinkoth J, Quilliam L, Cheng X (2002) Differential signaling of cyclic AMP—Opposing effects of exchange protein directly activated by cyclic AMP and cAMP-dependent protein kinase on protein kinase B activation. J Biol Chem 277:11497–11504. https://doi.org/10.1074/jbc.M110856200
10. Cheng X, Ji Z, Tsalkova T, Mei F (2008) EPAC and PKA: a tale of two intracellular cAMP receptors. Acta Biochim Biophys Sin (Shanghai) 40:651–662. https://doi.org/10.1111/j.1745-7270.2008.00438.x
11. de Rooij J, Zwartkruis FJ, Verheijen MH, Cool RH, Nijman SM, Wittinghofer A, Bos JL (1998) EPAC is a Rap1 guanine-nucleotide-exchange factor directly activated by cyclic AMP. Nature 396:474–477. https://doi.org/10.1038/24884
12. Kawasaki H, Springett GM, Mochizuki N, Toki S, Nakaya M, Matsuda M, Housman DE, Graybiel AM (1998) A family of cAMP-binding proteins that directly activate Rap1. Science 282:2275–2279. https://doi.org/10.1126/science.282.5397.2275
13. Schmidt M, Dekker FJ, Maarsingh H (2013) Exchange protein directly activated by cAMP (epac): a multidomain cAMP mediator in the regulation of diverse biological functions. Pharmacol Rev 65:670–709. https://doi.org/10.1124/pr.110.003707
14. Banerjee U, Cheng X (2015) Exchange protein directly activated by cAMP encoded by the mammalian rapgef3 gene: Structure, function and therapeutics. Gene 570:157–167. https://doi.org/10.1016/j.gene.2015.06.063
15. Sugawara K, Shibasaki T, Takahashi H, Seino S (2016) Structure and functional roles of EPAC2 (Rapgef4). Gene 575:577–583. https://doi.org/10.1016/j.gene.2015.09.029
16. Robichaux WG 3rd, Cheng X (2018) Intracellular cAMP Sensor EPAC: physiology, pathophysiology, and therapeutics development. Physiol Rev 98:919–1053. https://doi.org/10.1152/physrev.00025.2017
17. Yang W, Robichaux WG 3rd, Mei FC, Lin W, Li L, Pan S, White MA, Chen Y, Cheng X (2022) EPAC1 activation by cAMP regulates cellular SUMOylation and promotes the formation of biomolecular condensates. Sci Adv 8:eabm2960. https://doi.org/10.1126/sciadv.abm2960
18. Matic I, Schimmel J, Hendriks IA, van Santen MA, van de Rijke F, van Dam H, Gnad F, Mann M, Vertegaal AC (2010) Site-specific

identification of SUMO-2 targets in cells reveals an inverted SUMOylation motif and a hydrophobic cluster SUMOylation motif. Mol Cell 39:641–652. https://doi.org/10.1016/j.molcel.2010.07.026
19. Beauclair G, Bridier-Nahmias A, Zagury JF, Saïb A, Zamborlini A (2015) JASSA: a comprehensive tool for prediction of SUMOylation sites and SIMs. Bioinformatics 31:3483–3491. https://doi.org/10.1093/bioinformatics/btv403
20. Song J, Durrin LK, Wilkinson TA, Krontiris TG, Chen Y (2004) Identification of a SUMO-binding motif that recognizes SUMO-modified proteins. Proc Natl Acad Sci U S A 101:14373–14378. https://doi.org/10.1073/pnas.0403498101
21. Song J, Zhang Z, Hu W, Chen Y (2005) Small ubiquitin-like modifier (SUMO) recognition of a SUMO binding motif: a reversal of the bound orientation. J Biol Chem 280:40122–40129. https://doi.org/10.1074/jbc.M507059200
22. Mei FC, Cheng X (2005) Interplay between exchange protein directly activated by cAMP (EPAC) and microtubule cytoskeleton. Mol Biosyst 1:325–331. https://doi.org/10.1039/b511267b
23. Hendriks IA, D'Souza RC, Chang JG, Mann M, Vertegaal AC (2015) System-wide identification of wild-type SUMO-2 conjugation sites. Nat Commun 6:7289. https://doi.org/10.1038/ncomms8289
24. Meulmeester E, Kunze M, Hsiao HH, Urlaub H, Melchior F (2008) Mechanism and consequences for paralog-specific sumoylation of ubiquitin-specific protease 25. Mol Cell 30:610–619. https://doi.org/10.1016/j.molcel.2008.03.021
25. Zhu J, Zhu S, Guzzo CM, Ellis NA, Sung KS, Choi CY, Matunis MJ (2008) Small ubiquitin-related modifier (SUMO) binding determines substrate recognition and paralog-selective SUMO modification. J Biol Chem 283:29405–29415. https://doi.org/10.1074/jbc.M803632200
26. Liu C, Takahashi M, Li Y, Dillon TJ, Kaech S, Stork PJ (2010) The interaction of EPAC1 and Ran promotes Rap1 activation at the nuclear envelope. Mol Cell Biol 30:3956–3969. https://doi.org/10.1128/mcb.00242-10
27. Gloerich M, Vliem MJ, Prummel E, Meijer LA, Rensen MG, Rehmann H, Bos JL (2011) The nucleoporin RanBP2 tethers the cAMP effector EPAC1 and inhibits its catalytic activity. J Cell Biol 193:1009–1020. https://doi.org/10.1083/jcb.201011126
28. Pichler A, Gast A, Seeler JS, Dejean A, Melchior F (2002) The nucleoporin RanBP2 has SUMO1 E3 ligase activity. Cell 108:109–120. https://doi.org/10.1016/s0092-8674(01)00633-x
29. Cheng X, Yang W, Lin W, Mei F (2023) Paradoxes of cellular SUMOylation regulation: a role of biomolecular condensates? Pharmacol Rev. https://doi.org/10.1124/pharmrev.122.000784
30. Cheng X (2023) Protein SUMOylation and phase separation: partners in stress? Trends Biochem Sci 48:417–419. https://doi.org/10.1016/j.tibs.2022.12.003
31. Ni Z, Cheng X (2021) Origin and isoform specific functions of exchange proteins directly activated by cAMP: a phylogenetic analysis. Cells. https://doi.org/10.3390/cells10102750
32. Huang L, Weng X, Hofer F, Martin GS, Kim SH (1997) Three-dimensional structure of the Ras-interacting domain of RalGDS. Nat Struct Biol 4:609–615. https://doi.org/10.1038/nsb0897-609
33. Ponting CP, Benjamin DR (1996) A novel family of Ras-binding domains. Trends Biochem Sci 21:422–425. https://doi.org/10.1016/s0968-0004(96)30038-8
34. Li Y, Asuri S, Rebhun JF, Castro AF, Paranavitana NC, Quilliam LA (2006) The RAP1 guanine nucleotide exchange factor EPAC2 couples cyclic AMP and Ras signals at the plasma membrane. J Biol Chem 281:2506–2514. https://doi.org/10.1074/jbc.M508165200
35. Alenkvist I, Gandasi NR, Barg S, Tengholm A (2017) Recruitment of EPAC2A to insulin granule docking sites regulates priming for exocytosis. Diabetes 66:2610–2622. https://doi.org/10.2337/db17-0050
36. Liu C, Takahashi M, Li Y, Song S, Dillon TJ, Shinde U, Stork PJ (2008) Ras is required for the cyclic AMP-dependent activation of Rap1 via EPAC2. Mol Cell Biol 28:7109–7125. https://doi.org/10.1128/mcb.01060-08
37. Bacchelli E, Blasi F, Biondolillo M, Lamb JA, Bonora E, Barnby G, Parr J, Beyer KS, Klauck SM, Poustka A et al (2003) Screening of nine candidate genes for autism on chromosome 2q reveals rare nonsynonymous variants in the cAMP-GEFII gene. Mol Psychiatry 8:916–924. https://doi.org/10.1038/sj.mp.4001340
38. Srivastava DP, Woolfrey KM, Jones KA, Anderson CT, Smith KR, Russell TA, Lee H, Yasvoina MV, Wokosin DL, Ozdinler PH et al (2012) An autism-associated variant of EPAC2 reveals a role for Ras/EPAC2 signaling in controlling basal dendrite maintenance in mice. PLoS Biol 10:e1001350. https://doi.org/10.1371/journal.pbio.1001350
39. Berthouze-Duquesnes M, Lucas A, Saulière A, Sin YY, Laurent AC, Galés C, Baillie G, Lezoualc'h F (2013) Specific interactions between EPAC1, β-arrestin2 and PDE4D5 regulate β-adrenergic receptor subtype differential effects on cardiac hypertrophic signaling. Cell Signal 25:970–980. https://doi.org/10.1016/j.cellsig.2012.12.007
40. Rehmann H, Das J, Knipscheer P, Wittinghofer A, Bos JL (2006) Structure of the cyclic-AMP-responsive exchange factor EPAC2 in its auto-inhibited state. Nature 439:625–628. https://doi.org/10.1038/nature04468
41. Rehmann H, Arias-Palomo E, Hadders MA, Schwede F, Llorca O, Bos JL (2008) Structure of EPAC2 in complex with a cyclic AMP analogue and RAP1B. Nature 455:124–127. https://doi.org/10.1038/nature07187
42. Li S, Tsalkova T, White MA, Mei FC, Liu T, Wang D, Woods VL Jr, Cheng X (2011) Mechanism of intracellular cAMP sensor EPAC2 activation: cAMP-induced conformational changes identified by amide hydrogen/deuterium exchange mass spectrometry (DXMS). J Biol Chem 286:17889–17897. https://doi.org/10.1074/jbc.M111.224535
43. González-Prieto R, Eifler-Olivi K, Claessens LA, Willemstein E, Xiao Z, Talavera Ormeno CMP, Ovaa H, Ulrich HD, Vertegaal ACO (2021) Global non-covalent SUMO interaction networks reveal SUMO-dependent stabilization of the non-homologous end joining complex. Cell Rep 34:108691. https://doi.org/10.1016/j.celrep.2021.108691
44. Bhandari K, Cotten MA, Kim J, Rosen MK, Schmit JD (2021) Structure-function properties in disordered condensates. J Phys Chem B 125:467–476. https://doi.org/10.1021/acs.jpcb.0c11057
45. Iannucci LF, D'Erchia AM, Picardi E, Bettio D, Conca F, Surdo NC, Di Benedetto G, Musso D, Arrigoni C, Lolicato M et al (2023) Cyclic AMP induces reversible EPAC1 condensates that regulate histone transcription. Nat Commun 14:5521. https://doi.org/10.1038/s41467-023-41088-x
46. Qiao J, Mei FC, Popov VL, Vergara LA, Cheng X (2002) Cell cycle-dependent subcellular localization of exchange factor directly activated by cAMP. J Biol Chem 277:26581–26586. https://doi.org/10.1074/jbc.M203571200
47. Lee SY, Kang MG, Park JS, Lee G, Ting AY, Rhee HW (2016) APEX fingerprinting reveals the subcellular localization of proteins of interest. Cell Rep 15:1837–1847. https://doi.org/10.1016/j.celrep.2016.04.064
48. Zhu Y, Chen H, Boulton S, Mei F, Ye N, Melacini G, Zhou J, Cheng X (2015) Biochemical and pharmacological characterizations of ESI-09 based EPAC inhibitors: defining the ESI-09 "therapeutic window." Sci Rep 5:9344. https://doi.org/10.1038/srep09344

49. Brock M, Fan F, Mei FC, Li S, Gessner C, Woods VL Jr, Cheng X (2007) Conformational analysis of EPAC activation using amide hydrogen/deuterium exchange mass spectrometry. J Biol Chem 282:32256–32263. https://doi.org/10.1074/jbc.M706231200
50. Werner A, Moutty MC, Möller U, Melchior F (2009) Performing in vitro sumoylation reactions using recombinant enzymes. Methods Mol Biol 497:187–199. https://doi.org/10.1007/978-1-59745-566-4_12
51. Tatham MH, Rodriguez MS, Xirodimas DP, Hay RT (2009) Detection of protein SUMOylation in vivo. Nat Protoc 4:1363–1371. https://doi.org/10.1038/nprot.2009.128
52. Shevchenko A, Loboda A, Ens W, Schraven B, Standing KG (2001) Archived polyacrylamide gels as a resource for proteome characterization by mass spectrometry. Electrophoresis 22:1194–1203. https://doi.org/10.1002/1522-2683()22:6%3c1194::aid-elps1194%3e3.0.co;2-a
53. White MA, Tsalkova T, Mei FC, Cheng X (2019) Conformational states of exchange protein directly activated by cAMP (EPAC1) revealed by ensemble modeling and integrative structural biology. Cells. https://doi.org/10.3390/cells9010035
54. Webb B, Sali A (2021) Protein structure modeling with MODELLER. Methods Mol Biol 2199:239–255. https://doi.org/10.1007/978-1-0716-0892-0_14
55. Casañal A, Lohkamp B, Emsley P (2020) Current developments in coot for macromolecular model building of electron cryo-microscopy and crystallographic data. Protein Sci 29:1069–1078. https://doi.org/10.1002/pro.3791
56. Phillips JC, Hardy DJ, Maia JDC, Stone JE, Ribeiro JV, Bernardi RC, Buch R, Fiorin G, Hénin J, Jiang W et al (2020) Scalable molecular dynamics on CPU and GPU architectures with NAMD. J Chem Phys 153:044130. https://doi.org/10.1063/5.0014475
57. Humphrey W, Dalke A, Schulten K (1996) VMD: visual molecular dynamics. J Mol Graph 14(33–38):27–38. https://doi.org/10.1016/0263-7855(96)00018-5